



HAL
open science

Strong constitutive expression divergence among strains but no evidence of differential expression associated with sexual reproduction in *Alexandrium minutum*

Julie Seveno, Yasmine Even, Mickael Le Gac

► To cite this version:

Julie Seveno, Yasmine Even, Mickael Le Gac. Strong constitutive expression divergence among strains but no evidence of differential expression associated with sexual reproduction in *Alexandrium minutum*. *Harmful Algae*, 2020, 100, pp.101940. 10.1016/j.hal.2020.101940 . hal-03311940

HAL Id: hal-03311940

<https://hal.science/hal-03311940v1>

Submitted on 15 Dec 2022

HAL is a multi-disciplinary open access archive for the deposit and dissemination of scientific research documents, whether they are published or not. The documents may come from teaching and research institutions in France or abroad, or from public or private research centers.

L'archive ouverte pluridisciplinaire **HAL**, est destinée au dépôt et à la diffusion de documents scientifiques de niveau recherche, publiés ou non, émanant des établissements d'enseignement et de recherche français ou étrangers, des laboratoires publics ou privés.



Distributed under a Creative Commons Attribution - NonCommercial 4.0 International License

1 Strong constitutive expression divergence among strains but no
2 evidence of differential expression associated with sexual reproduction
3 in *Alexandrium minutum*.

4
5 Julie Seveno^{1,2}, Yasmine Even³, Mickael Le Gac^{1*}

6
7 ¹Ifremer, DYNECO PELAGOS, 29280 Plouzané, France

8 ²Laboratoire Mer Molécule Santé, Le Mans Université, 72000 Le Mans, France

9 ³Laboratoire des Sciences de l'Environnement Marin, UMR 6539 CNRS/UBO – Institut
10 Universitaire Européen de la Mer, Technopôle Brest-Iroise, 29280 Plouzané, France

11 *Corresponding author: mickael.le.gac@ifremer.fr

12
13 **Abstract**

14 Sexual reproduction remains poorly characterized in dinoflagellates. This is especially the case at the
15 molecular level. Here crossing experiments were performed among strains of the toxic dinoflagellate
16 *Alexandrium minutum* belonging to two genetically divergent groups. Gene expression was compared
17 between sexually compatible and incompatible crosses at the time of gamete fusion and resting cyst
18 (~zygote) formation. Not a single transcript was identified as differentially expressed between
19 compatible and incompatible crosses at these two crucial time points of the dinoflagellate life cycle.
20 However, several thousands of transcripts displayed constitutive expression differences between strains.
21 This was especially the case between the strains belonging to the genetically divergent groups. A few
22 hundreds of transcripts were also identified as differentially expressed between strains belonging to

23 opposite mating types. Some of these transcripts displayed homology with the *SxtA* protein, known to be
24 involved in saxitoxin production in cyanobacteria, as well as with proteins potentially involved in mating
25 in fungi.

26

27 **Keywords:** Sexual reproduction, *Alexandrium minutum*, Gene expression, Mating

28

29

30 **1. Introduction**

31 Sexual reproduction is almost universal in eukaryotes. In unicellular eukaryotes, species are either
32 homothallic when sex occurs between gametes produced by a single cell type, or heterothallic when two
33 sexually compatible cell types are required. In heterothallic species, sexual compatibility is determined
34 by mating types, encoded by mating-type locus (Russo et al. 2018; Hadjivasiliou and Pomiankowski
35 2016). The molecular bases of sexual reproduction remained unexplored in numerous unicellular
36 eukaryote phyla, which is especially true within dinoflagellates. This group of aquatic protists is famous
37 for its ability to form harmful algal blooms worldwide especially because some species produce toxins
38 that bio-accumulate in shellfish, but blooming algae also may clog animal gills or deplete oxygen
39 (Anderson et al. 2012a). Within dinoflagellates, the genus *Alexandrium* is one of the most prominent in
40 terms of toxic blooms, with numerous species producing several toxins, especially of the saxitoxin family
41 (Anderson et al. 2012b). This is the case of the genus type species, *A. minutum*, producing harmful algal
42 blooms worldwide. Like most dinoflagellates, *A. minutum* displays a haplontic life cycle, with cellular
43 division almost exclusively occurring in haploid cells (von Dassow and Montresor 2011). Sexual
44 reproduction occurs when haploid cells fuse, leading to the formation of diploid resting cysts (Figure 1).
45 Sexual compatibility and determinism remain poorly characterized in dinoflagellates, with systems
46 enabling self-fertilization (homothallism) or outcrossing (heterothallism). Homothallism has been

47 characterized in several species, for instance in the genus *Scrippsiella* (Montresor et al. 2003) or in the
48 species *A. taylora* (Giacobbe and Yang 1999). Several species display the ability to perform both homo-
49 and heterothallism. This is for instance the case of *Gymnodinium catenatum* (Figueroa et al. 2010) or
50 *Pheopolykrikos hartmannii* (Chai et al. 2020). Within the *Alexandrium* genus, several species, such as *A.*
51 *minutum* and *A. catenella*, seem to be strictly heterothallic, with complex compatibility systems involving
52 more than two mating types (Figueroa et al. 2007; Mardones et al. 2016).

53
54 In the present study, crossing experiments were performed among four strains of *A. minutum*,
55 associated with global gene expression profiling (RNA-seq), to investigate the molecular bases of sexual
56 reproduction within this species. For each of two genetic groups displaying evidence of independent
57 evolution and restricted gene flow based on >450,000 SNP markers (Le Gac et al. 2016), two strains
58 displaying opposite mating type were selected based on preliminary experiments. The experimental
59 design is summarized on Figure 2. Pairwise crosses were performed among the four strains. Global
60 expression profiling was performed: 1. when gamete fusions were observed in the sexually compatible
61 crosses, i.e two days after initial contact; 2. when resting cysts were first observed in the sexually
62 compatible crosses, i.e. 5 days after initial contact; and 3. for clonal controls. Reproductive success was
63 quantified by counting the number of resting cysts ten days after initial contact. Following this
64 experimental design, the following questions were asked: 1. Is there sexual compatibility among the two
65 genetic groups? 2. What are the genes displaying differential expression at the time of gamete fusion
66 and at the time of encystment? 3. What is the level of constitutive expression among strains and are
67 there mating type specific expression patterns?

68

69 **2. Material and methods**

70 **2.1. Experimental design**

71 Crossing experiments and RNAseq analyses were performed using four strains. The strains correspond to
72 clonal cultures initiated after micro-pipetting individual cells from natural samples.

73 Strains were grown in K medium for 10 days (corresponding to the end of the exponential phase) and
74 diluted in their own culture filtrate (0.2 μ m) in order to obtain an initial cell density of 5,000 cells per mL.

75 All pairwise crosses as well as clonal controls were performed in serial triplicates (all crosses from
76 replicate one initiated in parallel on a given day, all crosses from replicate two initiated in parallel on
77 another day...). All cultures were performed at 18°C, under a 12:12 L:D cycle and
78 80 μ mol photons $m^{-2} s^{-1}$, in algal incubators. To quantify reproductive success, for each pairwise cross, 1
79 mL of each strain was mixed in 24 well plates. In order to extract RNA, for each pairwise cross, 75 mL of
80 each strain was mixed in flasks. Preliminary crossing experiments indicated that, in case of sexual
81 compatibility, cell fusion occurred after 2 days and the first permanent cysts were observed after 5 days.

82 Sexual reproduction was quantified using an inverted microscope, after 10 days, by counting resting
83 cysts remaining at the bottom of the 24 well plates after washing the plates twice with sterile sea water.

84 RNA extraction was performed after 2 days and 5 days from the same flask (Figure 2A), and we verified
85 that the first resting cyst appeared after 5 days. For clonal controls, RNA extraction was only performed
86 after 2 days. There was a total of 48 RNA samples. Samples are summarized in Figure 2B and in
87 Supplementary table 1. The strains Am231 and Am233 were isolated from the Bay of Concarneau
88 (France) in 2010, the strain Am1106 was isolated from Cork Harbor (Ireland) in 2010, and the strain
89 Am1249 was isolated from the Bay of Brest (France) in 2013. Strains Am231 and 233 belong to *A.*
90 *minutum* genetic group B. Strains Am1106 and Am1249 belong to *A. minutum* genetic group A (Le Gac et
91 al. 2016). Mating type determination was based on a preliminary crossing experiment assessing the
92 global pattern of sexual compatibility among ten *A. minutum* strains which suggested the occurrence of
93 only two mating types in the tested strains (Supplementary Table 2).

94

95 2.2. RNA extraction library preparation and sequencing

96 For RNA extraction, cultures were centrifuged at 4500 g for 8 min and sonicated on ice for 30 s in LBP
97 buffer (Macherey-Nagel, Duren, Germany). Extraction was performed using NucleoSpin® RNA Plus kit
98 (Macherey-Nagel) following the manufacturer's protocol. Extracted RNA was quantified using a Biotek
99 Epoch spectrophotometer and the quality estimated on RNA 6000 nanochips using a Bioanalyzer (Agilent
100 Technologies, Palo Alto, CA). Library preparation was performed using the Illumina mRNA TruSeq
101 stranded kit starting from 0.5 µg of total RNA. Library quality was assessed on a Bioanalyzer using high-
102 sensitivity DNA analysis chips and quantified using Kappa Library Quantification Kit. Paired-end
103 sequencing was performed using 2 x 150 bp cycles on Illumina Hiseq3000 at the GeT-PlaGe France
104 Genomics sequencing platform (Toulouse, France). The 48 samples were sequenced on 2 lanes
105 (multiplex 24).

106

107 2.3. Bioinformatic analyses

108 Prior to read mapping, raw reads were initially characterized with FastQC
109 (<http://www.bioinformatics.bbsrc.ac.uk/projects/fastqc/>) and Trimmomatic (V. 0.33; Bolger et al., 2014)
110 was used to trim ambiguous, low quality reads and sequencing adapters with parameters
111 ILLUMINACLIP:Adapters.fasta:2:30:10, LEADING:3, TRAILING:3, MAXINFO:80:0.8 and MINLEN:70. These
112 parameters enable: 1. To remove Illumina adapters; 2. To remove leading and trailing low quality bases;
113 3. To perform an adaptive quality trim balancing read length benefits with a target read length of 80
114 bases and sequencing error costs with a strictness factor of 0,8 (favoring read correctness); 4. To remove
115 reads < 70 bases long after the previous steps.

116 A reference transcriptome previously assembled using 18 *A. minutum* strains, including the strains used
117 in the present study was considered (Le Gac et al., 2016). This 153,222 transcripts reference, for a total
118 of 117,601,765 bp, was annotated using UNIPROT/Swissprot (<https://www.uniprot.org/>) database and

119 classified in Gene Ontology categories (GO; <http://geneontology.org/>) as described in Le Gac et al.
120 (2016). Additional homology analyses were performed for transcripts displaying differential expression:
121 first analysis: between strains displaying opposite mating types (as identified based on global
122 compatibility patterns following preliminary crossing assays, Supplementary Table 2) and second
123 analysis: between strains displaying opposite mating types and giving rise to the formation of resting
124 cysts (named compatible strains hereafter; see results and supplementary Table 1). For these two sets of
125 transcripts, an additional blastx analysis was performed against the nr ncbi database and against a subset
126 of the nr database only containing the sequences with “mating” or “Mating” in the sequence description
127 section. The reference transcriptome from Le Gac et al. (2016) was assembled using strains reproducing
128 asexually at the time of RNA extraction. A second reference transcriptome was assembled de novo using
129 Trinity (Haas et al. 2013) after pooling the reads of the 48 samples obtained in the present study. This
130 was done to ensure that transcripts potentially specifically expressed during sexual reproduction are
131 considered in the differential expression analysis. From read mapping to differential expression analysis
132 (see below), all the analyses were performed using the two reference transcriptomes. As results were
133 similar with both reference transcriptomes, only the results obtained using the reference transcriptome
134 from Le Gac et al. (2016) are presented. Trimmed reads were aligned to the reference transcriptome
135 using BWA-MEM (Burrows-Wheeler Alignment Tool; Li and Durbin, 2009). Only reads with a mapping
136 score >10 were retained. Pairs for which the two reads did not map concordantly on the same transcript
137 were removed. Samtools was used to sort, index, and obtain raw read count table from bam files (Li et
138 al. 2009).

139

140 2.4. Differential expression analyses

141 Independent analyses were performed after removing transcripts with a total read count equal to zero
142 (149,144 transcripts considered) and transcripts with an average read count per sample lower than 10

143 (140,474 transcripts considered). As the two analyses gave similar results, results are only given for the
144 second one. The raw read count table was transformed using the Variance Stabilizing Transformation
145 (vst), and the gene expression variability across samples explored using a Principal Component Analysis
146 (PCA). Differential expression (DE) analyses were performed using negative binomial models on raw read
147 counts using Wald tests as implemented in DESeq2 (Love et al. 2014) and using linear models on voom
148 normalized read counts as implemented in limma (Ritchie et al. 2015). Transcripts were considered as
149 differentially expressed after false discovery rate (FDR) adjustment when q-values were < 0.1 using both
150 approaches. Five types of DE analyses were performed. They all involved a simple statistical design with
151 a single factor and two groups. More complex statistical designs involving multiple factors and
152 interaction terms were also explored but did not lead to robust results and were therefore discarded
153 (data not shown). The first type of analyses was performed to identify transcripts DE when two strains
154 are interacting in the same culture. For each pair of strains, at day 2, the expression levels quantified
155 when the two clones have been in the same culture for 2 days and when the two clones have been in
156 two separate cultures for two days were compared. This later condition was obtained by adding, for
157 each pair of strains and each replicate, the read count table of the clonal controls after correcting for
158 library size differences (contact tests; Figure 2 C1; Supplementary table 3). The second type of analyses
159 was performed to identify, for each pair of clones, the transcripts DE between day two and five (day 2 vs
160 day 5 tests; Figure 2 C2; Supplementary table 3). Third and fourth, expression was compared between
161 sexually compatible and incompatible crosses at day 2 (compatibility day 2 tests ; Figure 2 C3 ;
162 Supplementary table 3) and at day 5 (compatibility day 5 tests ; Figure 2 C4 ; Supplementary table 3). For
163 these third and fourth analyses, the read count tables of the replicates for a given type of cross were
164 summed and the different types of compatible crosses were considered as replicates. Based on the
165 resting cyst quantification crosses Am231 * Am233, Am1106 * Am1249, and Am233 * Am1106 were
166 considered as compatible and crosses Am231 * Am1249, Am233 * Am1249, and Am231 * Am1106 as

167 incompatible (see Results). Fifth, expression was compared between pairs of strains when cultivated
168 separately (strain tests; Figure 2 C5; Supplementary table 3). Overlap between sets of DE transcripts was
169 analyzed using upsetR R package (Conway et al. 2017).

170

171 **3. Results**

172 **3.1. Quantifying reproductive success**

173 Crosses were performed between four strains of *A. minutum* and the number of resting cysts was
174 quantified after ten days of contact. Our results indicated that crosses Am231 * Am233, Am1106 *
175 Am1249, and Am233 * Am1106 produced resting cysts and were sexually compatible, while crosses
176 Am231 * Am1249, Am233 * Am1249, and Am231 * Am1106 did not produce resting cysts (Figure 3). For
177 sexually compatible crosses, gamete fusion was observed at day 2 and the first resting cysts were
178 observed at day 5.

179 **3.2. Differential expression during sexual reproduction**

180 Gene expression was quantified two days and five days after initial contact between strains as well as
181 two days after inoculation for clonal controls. Gene expression variability was explored using a PCA
182 analysis, (Figure 4).

183 Four types of DE analyses were performed to identify genes DE during sexual reproduction and more
184 precisely during gamete fusion and the formation of resting cysts. The first analysis was performed to
185 identify DE linked to the actual interaction between strains. For each pairwise cross, expression
186 quantified after two days of contact was compared to the expression quantified in the clonal controls. As
187 indicated Figure 5, not a single transcript was identified as differentially expressed. It was the case for
188 the sexually compatible (Am231 * Am233, Am1106 * Am1249, and Am233 * Am1106) as well as sexually
189 incompatible (Am231 * Am1249, Am233 * Am1249, and Am231 * Am1106) crosses. The second type of
190 DE analysis was performed to identify transcripts DE between two and five days. Here again not a single

191 transcript was identified as differentially expressed (Figure 6). The third and fourth types of DE analyses
192 were performed to identify transcripts DE during gamete fusion and preceding encystment. Here again,
193 not a single transcript was identified as differentially expressed (Figure 7).

194 **3.3. Constitutive differential expression between strains**

195 A fifth type of DE analysis was performed to identify transcripts DE between strains, by comparing the
196 expression of the clonal controls. A strong DE between strains was observed, with between 6,458 and
197 19,616 transcripts identified as DE (Figure 8). The overlap between sets of transcripts DE in pairwise
198 fashion is indicated on Figure 9. A total of 2389 transcripts were systematically DE between strains
199 belonging to genetic groups A and B (Figure 9, orange barplot). Strain specific DE was identified with
200 1335, 1359, 1779 and 1785 transcripts displaying systematic DE in Am233, Am231, Am1106 and
201 Am1249, respectively (Figure 9, purple barplots). Interestingly, regarding mating type differentiation, 298
202 transcripts were found systematically DE between strains displaying opposite mating types (Am231 and
203 Am1106 corresponding to mating type + and Am233 and Am1249 corresponding to mating type -; Figure
204 9, red barplot). Among these transcripts 183 were more expressed in mating type + strains and 115 were
205 more expressed in mating type - strains. A total of 41 transcripts displayed homology with proteins
206 belonging to the manually annotated UniProt/SwissProt database. Following additional blastx homology
207 search against the nr ncbi database, two additional transcripts were identified as displaying homology
208 with a protein known to be involved in saxitoxin production (*SxtA*). In addition, seven transcripts
209 displayed homology with proteins potentially involved in mating in other organisms (Table 1,
210 Supplementary Table4). Finally, there were only 43 transcripts systematically DE between strains
211 displaying opposite mating types and which crosses lead to the formation of resting cysts
212 (Am231*Am233, Am1106*Am1249, Am233*Am1106; not shown on Figure 9). Among these transcripts,
213 27 were more expressed in mating type + strains and 16 mating type - strains. A total of 6 transcripts
214 were annotated (Table 2, Supplementary Table5).

215

216 **4. Discussion**

217 In the present study, crossing experiments were performed among four strains belonging to two genetic
218 groups of the toxic dinoflagellate *A. minutum*.

219 The first main result of the study was the observation of sexual reproduction among strains belonging to
220 two genetic groups. In a previous study (Le Gac et al. 2016), two divergent genetic groups were identified
221 within *A. minutum*, and population genomic simulations suggested a restricted gene flow among them.

222 Here, the ability to obtain resting cysts from crosses involving strains from the two genetic groups shows
223 that they recognize each other as potential sexual partners and display sexual compatibility enabling the
224 formation of resting cysts (~zygotes). However, this result should not be taken as an evidence for an
225 absence of reproductive isolation among the two groups, as reproductive isolation may involve
226 postzygotic incompatibilities (inability to produce viable or fertile offspring) or environmental based
227 reproductive isolation (that may for instance result from differences in phenology or geographic
228 repartition; Coyne and Orr 2004). One of the two inter-genetic crosses led to the formation of resting
229 cysts while the other did not seem to produce resting cyst. At first sight this result may suggest an
230 asymmetric reproductive isolation (compatible A/- * B/+ crosses vs incompatible A/+ * B/- crosses).
231 However, *A. minutum* displays a complex compatibility system involving more than two mating types
232 (Figuroa et al. 2007). As a result, the observed asymmetry may be incidental and investigating putative
233 asymmetric reproductive isolation would require performing crosses among numerous strains.

234 The second notable result is the total absence of differential expression during sexual reproduction at
235 the time of gamete fusion as well as at the time of encystment. Dinoflagellates display numerous
236 peculiar genomic characteristics among which the presence of spliced-leader (SL) sequences at the 5'
237 end of most mature mRNA, suggesting that transcription in dinoflagellates may be strongly influenced by
238 SL-trans-splicing mechanisms (Zhang et al. 2007). As indicated by previous studies, dinoflagellates

239 polyadenylated mRNA levels are indeed rather stable with very few genes displaying differential
240 expression across conditions (Roy et al. 2018). A possible explanation for the absence of observed
241 differential expression could be that regulation occurs at the translation level and neither during
242 transcription nor during mRNA maturation leading to polyadenylated mRNA. An alternative explanation
243 would be that at the time of RNA extraction only a very small proportion of cells is actually involved in
244 sexual reproduction, potentially resulting in the sexual reproduction specific expression pattern being
245 too diluted to be detected at the population scale. Indeed, neglecting cell division and mortality, in the
246 most successful crosses, about 2/5 of the initial cells ended up involved in sexual reproduction leading to
247 the formation of a resting cyst (2500 cells.ml⁻¹ of each partner were initially mixed and about 1000
248 resting cysts.ml⁻¹ were obtained), but the proportion of cells actually involved in sexual reproduction at
249 the time of RNA extraction remains unknown. However, the presence of a sexually compatible partner
250 could have triggered gene expression responses even in cells that are not involved in gamete fusion or
251 encystment at the time of RNA extraction. As a matter of comparison, similar experimental designs
252 performed in diatoms led to the identification of more than a thousand differentially expressed genes
253 during sexual reproduction (Basu et al. 2017; Ferrante et al. 2019). A last element that could explain why
254 differential expression during sexual reproduction in *A. minutum* was not identified may be linked to the
255 strong constitutive expression among strains (see below). Such massive strain specific expression could
256 mask moderate expression responses. To test this hypothesis, allele specific gene expression analyses
257 were performed based on variable SNPs covering 21,000 transcripts (data not shown). Even using this
258 approach, enabling the independent gene expression monitoring of each strain in a given pairwise cross,
259 no differentially expressed transcript was identified.

260 The last and probably most notable result of the study was the identification of massive strain specific
261 differential expression both in terms of number of transcripts and fold change. Differential expression
262 between strains belonging to the two *A. minutum* genetic groups was identified previously (Le Gac et al.

263 2016) and was confirmed in the present study with between 7 and 13% of transcripts displaying
264 differential expression. Within the genetic groups, strain specific differential expression affected 4-6% of
265 the transcripts, which is totally in line with a previous study in *A. minutum* (4% of differentially expressed
266 transcripts between strains; Yang et al. 2010) and *A. fundyense* (5%; Wohlrab et al. 2016). The molecular
267 mechanism underlying the extreme differential expression pattern observed among strains, as well as
268 the functional consequences of such differences remain to be explored.

269 A few hundreds of transcripts were differentially expressed between the *A. minutum* strains displaying
270 opposite mating types. The present study was not designed to specifically determine mating type specific
271 expression patterns. This would require investigating differential expression among numerous strains
272 displaying opposite mating types. However, some of these transcripts displayed notable homology with
273 proteins potentially involved in mating in other organisms. Indeed, two transcripts displayed homology
274 with genes involved in mating through transfer of environmental signals involving G-protein receptors
275 and MAPK signaling pathways, respectively. The first one corresponded to the beta subunit of a mating
276 factor receptor-coupled G protein (Yang et al, 2012). In the yeast *Saccharomyces cerevisiae*, the G
277 protein $\beta\gamma$ subunit is involved in the pheromone response pathway by activating signal transduction
278 cascades involved in mating (Whiteway et al. 1995; Pryciak and Huntress, 1998). This candidate is
279 especially interesting because, unlike what has been described in yeast, it might be sex specific in *A.*
280 *minutum*. The second one, corresponded to the MAPKKK, which is part of the Mitogen-Activated Protein
281 Kinase (MAPK) signaling pathways, one of the most important and evolutionarily conserved mechanisms
282 to detect extracellular information in all eukaryotes. Another interesting transcript displayed homology
283 with the JEM1p DnaJ-like chaperone located in the endoplasmic reticulum of yeast, *Saccharomyces*
284 *boulardii* and *S. cerevisiae*. Several studies have shown that the Δ jem1 mutant was defective in nuclear
285 fusion during mating suggesting a key role in karyogamy during mating (Nishikawa and Endo 1997, 1998).
286 Another candidate potentially associated with mating displayed homology with the Ste20 (Sterile) like

287 protein kinase. This serine-threonine kinase is a member of the Ste20 related protein kinase family. This
288 large protein family includes PAKs (p21 activated kinases) and GCKs (germinal centre kinases) and is
289 known to be involved in mating. The Ste20-related kinases function in a MAP kinase signaling cascade
290 and they control the mating and differentiation in the *Cryptococcus neoformans* fungus. Especially, Ste20
291 and Pak1 have been shown to play crucial roles in polarized morphogenesis at different steps during
292 mating: namely cell fusion and polarity maintenance in the heterokaryotic mating filament (Nichols et
293 al., 2004). They also have important roles in actin-mediated polarized growth. For example, deletion of
294 Ste20 (*PAK1*) in the basidiomycete yeast *Cryptococcus neoformans* results in reduced mating-related
295 filamentation (Wang et al., 2002). The last candidate potentially involved in mating is Pry1 (pathogen
296 related in yeast) and together with Pry2 and Pry3, they belong to the CAP superfamily and are involved
297 in sterol secretion in yeast cells (Darwiche et al., 2016). Among the Pry proteins only Pry3 has been
298 demonstrated to influence mating in yeast *S. cerevisiae* (Darwiche et al., 2018). Finally, of special
299 interest, two transcripts displaying mating type specific expression pattern were homologous to *SxtA*, a
300 protein known to be involved in saxitoxin production in cyanobacteria and with several known homologs
301 in the *Alexandrium* genera (Hackett et al. 2013). Although this remains highly speculative, saxitoxin has
302 been previously proposed to act as sex pheromone in *Alexandrium* (Wyatt and Jenkinson 1997; Cusick
303 and Sayler 2013), and genetic differences between diverging *A. minutum* populations have been
304 previously characterized (Le Gac et al. 2016).

305

306 **5. Conclusion**

307 The present study highlights two main results. The first one is a negative result with no evidence of
308 differential expression associated with sexual reproduction in *A. minutum* that may directly result from
309 dinoflagellate molecular peculiarities in terms of transcriptional regulation. Second, a strong constitutive
310 expression difference among strains was identified, but the functional consequences of these differences

311 remain to be explored. Finally, some transcripts with mating type specific expression patterns displayed
312 homology with proteins known to be involved in toxin production in cyanobacteria or mating in fungi.

313

314

315 Acknowledgements

316 This work was supported by a financial support from Ifremer. We acknowledge Pascale Malestroit for
317 crossing experiment, Julien Quéré for RNA extraction and library preparation, GetPlage for sequencing,
318 SebiMer for bioinformatics support, and three anonymous reviewers for constructive comments.

319

320 Author contributions

321 MLG designed research; JS, YE and MLG analyzed the data and wrote the manuscript.

322

323 Competing interests

324 The authors declare no competing interests.

325

326 Data availability

327 Raw reads from the transcriptomic dataset are available ([https://doi.org/10.12770/f721cb44-3792-472f-](https://doi.org/10.12770/f721cb44-3792-472f-acab-95833c401c7c)
328 [acab-95833c401c7c](https://doi.org/10.12770/f721cb44-3792-472f-acab-95833c401c7c)).

329

330

331 **References**

332 Anderson, D.M., Alpermann, T.J., Cembella, A.D., Collos, Y., Masseret, E. and Montresor, M., 2012a. The
333 globally distributed genus *Alexandrium*: Multifaceted roles in marine ecosystems and impacts on
334 human health. *Harmful Algae* 14, 10-35.

- 335 Anderson, D.M., Cembella, A.D. and Hallegraeff, G.M., 2012b. Progress in Understanding Harmful Algal
336 Blooms: Paradigm Shifts and New Technologies for Research, Monitoring, and Management, in:
337 Carlson, C.A. and Giovannoni, S.J. (Eds.), Annual Review of Marine Science, Vol 4. Annual Reviews,
338 Palo Alto, pp. 143-176.
- 339 Basu, S., Patil, S., Mapleson, D., Russo, M.T., Vitale, L., Fevola, C., Maumus, F., Casotti, R., Mock, T.,
340 Caccamo, M., Montresor, M., Sanges, R. and Ferrante, M.I., 2017. Finding a partner in the ocean:
341 molecular and evolutionary bases of the response to sexual cues in a planktonic diatom. *New*
342 *Phytologist* 215, 140-156.
- 343 Bolger A.M., Lohse M., Usadel B. 2014. Trimmomatic: a flexible trimmer for Illumina sequence data.
344 *Bioinformatics* 30, 2114-2120.
- 345 Chai, Z., Hu, Z., Liu, Y. and Tang, Y. 2020. Proof of homothally of *Pheopolykrikos hartmannii* and details of
346 cyst germination process. *J. Ocean. Limnol.* 38, 114–123.
- 347 Conway, J.R., Lex, A. and Gehlenborg, N., 2017. UpSetR: an R package for the visualization of intersecting
348 sets and their properties. *Bioinformatics* 33, 2938-2940.
- 349 Coyne JA and Orr HA. 2004. Speciation. Sinauer Associates, Inc. Sunderland, Massachusetts USA.
- 350 Cusick, K.D. and Sayler, G.S., 2013. An Overview on the Marine Neurotoxin, Saxitoxin: Genetics,
351 Molecular Targets, Methods of Detection and Ecological Functions. *Marine Drugs* 11, 991-1018.
- 352 Darwiche R., El Atab O., Cottier S., Schneider R., 2018. The function of yeast CAP family proteins in lipid
353 export, mating, and pathogen defense. *FEBS Letters* 8, 1304-1311.
- 354 Darwiche R., Kelleher A., Hudspeth E.M., Schneider R., Asojo O.A., 2016. Structural and functional
355 characterization of the CAP domain of pathogen-related yeast 1 (Pry1) protein. *Scientific Reports*
356 6, 28838.
- 357 Ferrante, M.I., Entrambasaguas, L., Johansson, M., Topel, M., Kremp, A., Montresor, M. and Godhe, A.,
358 2019. Exploring Molecular Signs of Sex in the Marine Diatom *Skeletonema marinoi*. *Genes* 10.

- 359 Figueroa, R.I., Garces, E. and Bravo, I., 2007. Comparative study of the life cycles of *Alexandrium*
360 *tamutum* and *Alexandrium minutum* (Gonyaulacales, Dinophyceae) in culture. *Journal of*
361 *Phycology* 43, 1039-1053.
- 362 Figueroa, R.I., Rengefors, K., Bravo, I., Bens, S. 2010. From homothally to heterothally: Mating
363 preferences and genetic variation within clones of the dinoflagellate *Gymnodinium catenatum*.
364 *Deep-Sea Research II* 57 190–198.
- 365 Giacobbe M. G., Yang X. 1999. The life history of *Alexandrium taylori* (Dinophyceae). *Journal of Phycology*
366 35, 331-338.
- 367 Haas, B., Papanicolaou, A., Yassour, M. et al. 2013. De novo transcript sequence reconstruction from
368 RNA-seq using the Trinity platform for reference generation and analysis. *Nat Protoc* 8, 1494–
369 1512.
- 370 Hackett, J.D., Wisecaver, J.H., Brosnahan, M.L., Kulis, D.M., Anderson, D.M., Bhattacharya, D., Plumley,
371 F.G. and Erdner, D.L., 2013. Evolution of Saxitoxin Synthesis in Cyanobacteria and Dinoflagellates.
372 *Molecular Biology and Evolution* 30, 70-78.
- 373 Hadjivasiliou, Z. and Pomiankowski, A., 2016. Gamete signalling underlies the evolution of mating types
374 and their number. *Philosophical Transactions of the Royal Society B-Biological Sciences* 371.
- 375 Le Gac, M., Metegnier, G., Chomerat, N., Malestroit, P., Quere, J., Bouchez, O., Siano, R., Destombe, C.,
376 Guillou, L. and Chapelle, A., 2016. Evolutionary processes and cellular functions underlying
377 divergence in *Alexandrium minutum*. *Molecular Ecology* 25, 5129-5143.
- 378 Li H., Handsaker B., Wysoker A., Fennell T., Ruan J., Homer N., Marth G., Abecasis G., Durbin R., and 1000
379 Genome Project Data Processing Subgroup. 2009, The Sequence alignment/map (SAM) format and
380 SAMtools, *Bioinformatics* 25,2078-9.
- 381 Love, M.I., Huber, W. & Anders, S. 2014. Moderated estimation of fold change and dispersion for RNA-
382 seq data with DESeq2. *Genome Biol* 15, 550.

- 383 Mardones, J.I., Bolch, C.J., Guzman, L., Paredes, J., Varela, D., G M. Hallegraeff, G.M. 2016. Role of resting
384 cysts in Chilean *Alexandrium catenella* dinoflagellate blooms revisited. *Harmful Algae* 55, 238-249.
- 385 Montresor, M., Sgroso, S., Procaccini, G. and Kooistra, W. H. C. F. 2003. Intraspecific diversity in
386 *Scrippsiella trochoidea* (Dinophyceae): evidence for cryptic species. *Phycologia* 42, 56-70.
- 387 Nichols C.B., Fraser J.A., Heitman J. 2004. PAK kinases Ste20 and Pak1 govern cell polarity at different
388 stages of mating in *Cryptococcus neoformans*. *Molecular Biology of the Cell* 10, 4476-4489.
- 389 Nishikawa S., Endo T., 1997. The yeast JEM1p is a DnaJ-like protein of the endoplasmic reticulum
390 membrane required for nuclear fusion. *Journal of Biological Chemistry* 20, 12889-12892.
- 391 Nishikawa S., Endo T., 1998. Reinvestigation of the functions of the hydrophobic segment of Jem1p, a
392 yeast endoplasmic reticulum membrane protein mediating nuclear fusion. *Biochemical and*
393 *Biophysical Research Communications* 3, 785-789.
- 394 Pryciak P.M., Huntress F.A., 1998. Membrane recruitment of the kinase cascade scaffold protein Ste5 by
395 the Gbetagamma complex underlies activation of the yeast pheromone response pathway. *Genes*
396 *& Development* 17, 2684-2697.
- 397 Ritchie M.E., Phipson B., Wu D., Hu Y., Law C.W., Shi W., Smyth G.K. 2015. limma powers differential
398 expression analyses for RNA-sequencing and microarray studies. *Nucleic Acids Research*. 43, e47.
- 399 Roy, S., Jagus, R. and Morse, D., 2018. Translation and Translational Control in Dinoflagellates.
400 *Microorganisms* 6.
- 401 Russo, M.T., Vitale, L., Entrambasaguas, L., Anestis, K., Fattorini, N., Romano, F., Minucci, C., De Luca, P.,
402 Biffali, E., Vyverman, W., Sanges, R., Montresor, M. and Ferrante, M.I., 2018. MRP3 is a sex
403 determining gene in the diatom *Pseudo-nitzschia multistriata*. *Nature Communications* 9.
- 404 von Dassow, P. and Montresor, M., 2011. Unveiling the mysteries of phytoplankton life cycles: patterns
405 and opportunities behind complexity. *Journal of Plankton Research* 33, 3-12.

- 406 Walker L. (1984). Life histories, dispersal, and survival in marine, planktonic dinoflagellates. In: Steidinger
407 K. & Walker L. (eds.), *Marine Plankton Life Cycle Strategies*, CRC Press.
- 408 Wang P., Nichols C.B., Lengeler K.B., Cardenas M.E., Cox G.M., Perfect J.R., Heitman J., 2002. Mating-
409 type-specific and nonspecific PAK kinases play shared and divergent roles in *Cryptococcus*
410 *neoformans*. *Eukaryotic Cell* 12, 257-272.
- 411 Whiteway M.S., Wu C., Leeuw T., Clark K., Fourest-Lieuvin A., Thomas D.Y., Leberer E., 1995. Association
412 of the yeast pheromone response G protein beta gamma subunits with the MAP kinase scaffold
413 Ste5p. *Science* 230, 1572-1575. Wisecaver, J.H. and Hackett, J.D., 2011. Dinoflagellate Genome
414 Evolution. *Annual Review of Microbiology*, Vol 65 65, 369-387.
- 415 Wohlrab, S., Tillmann, U., Cembella, A. and John, U., 2016. Trait changes induced by species interactions
416 in two phenotypically distinct strains of a marine dinoflagellate. *ISME Journal* 10, 2658-2668.
- 417 Wyatt, T. and Jenkinson, I.R., 1997. Notes on *Alexandrium* population dynamics. *Journal of Plankton*
418 *Research* 19, 551-575.
- 419 Yang, I., John, U., Beszteri, S., Glockner, G., Krock, B., Goesmann, A. and Cembella, A.D., 2010.
420 Comparative gene expression in toxic versus non-toxic strains of the marine dinoflagellate
421 *Alexandrium minutum*. *BMC Genomics* 11.
- 422 Yang R.Y., Li H.T., Zhu H., Zhou G.P., Wang M., Wang L., 2012. Draft genome sequence of CBS 2479, the
423 standard type strain of *Trichosporon asahii*. *Eukaryotic Cell* 11, 1415-1416.
- 424 Zhang, H., Hou, Y., Miranda, L., Campbell, D.A., Sturm, N.R., Gaasterland, T. and Lin, S., 2007. Spliced
425 leader RNA trans-splicing in dinoflagellates. *Proceedings of the National Academy of Sciences of*
426 *the United States of America* 104, 4618-4623.

427 Table 1: Annotated transcripts DE between strains displaying opposite mating types

Transcripts	Average expression	fold change (log ₂ (MT+/MT-))	Transcript length	Homolog
comp103401_c0_seq2	349	0,50	1503	Uncharacterized protein DKFZp434B061 (Swissprot)
comp108403_c0_seq1	243	0,95	1648	Probable serine/threonine-protein kinase DDB_G0275165 (Swissprot)
comp109153_c0_seq1	291	0,78	1587	Ubiquinone biosynthesis O-methyltransferase (Swissprot)
comp111017_c0_seq1	229	1,27	1350	Pentatricopeptide repeat-containing protein At2g15630, mitochondrial (Swissprot)
comp111238_c0_seq1	429	0,71	1483	Cathepsin E (Swissprot)
comp111675_c1_seq1	546	-0,59	1273	Sterol 3-beta-glucosyltransferase UGT80A2 (Swissprot)
comp111818_c0_seq1	67	0,72	431	Elongation factor 1-alpha (Swissprot)
comp111943_c1_seq1	318	-1,68	1873	Protein MEI2-like 5 (Swissprot)
comp112946_c0_seq4	529	-2,07	3219	Eukaryotic translation initiation factor isoform 4G-2 (Swissprot)
comp113432_c0_seq1	227	1,75	1489	Protein MEI2-like 4 (Swissprot)
comp113671_c0_seq4	112	-1,00	1185	Protein MEI2-like 2 (Swissprot)
comp116500_c0_seq1	689	-1,10	1699	Mitogen-activated protein kinase 4 (Swissprot) Mitogen-activated serine/threonine protein kinase involved in mating, putative(mating)
comp117201_c0_seq1	243	-0,77	1535	Carbohydrate-binding domain-containing protein C2E1P3.05c (Swissprot)
comp117501_c0_seq1	146	-1,07	1133	SxtA long isoform, partial (nr)
comp118887_c0_seq1	1330	-0,94	2628	related to Ste20-like protein kinase; has effect on mating (mating)
comp119307_c0_seq1	810	0,57	3713	related to Ste20-like protein kinase; has effect on mating (mating)
comp120037_c0_seq1	306	-0,80	1371	D-xylose 1-dehydrogenase (NADP(+)) 2 (Swissprot)
comp124887_c0_seq1	895	-0,64	2745	Sterol 3-beta-glucosyltransferase (Swissprot)
comp125166_c0_seq1	210	-0,82	1252	Uncharacterized protein y4mH (Swissprot)
comp125447_c0_seq1	74	0,92	1524	Ribulose biphosphate carboxylase (Swissprot)
comp125574_c0_seq2	459	0,54	1738	Protein PRY1 (Swissprot) Similar to Saccharomyces cerevisiae YJL078C PRY3 Cell wall protein with a role in mating efficiency (mating)
comp127738_c0_seq1	421	0,54	2645	Cytosine-specific methyltransferase NlaX (Swissprot)
comp127932_c1_seq2	228	-1,40	1756	SxtA short isoform precursor (nr)

comp128115_c0_seq1	175	0,57	1463	Ribosomal RNA large subunit methyltransferase I (Swissprot)
comp130909_c0_seq1	449	1,08	1881	Pentatricopeptide repeat-containing protein At5g04810, chloroplastic (Swissprot)
comp132966_c2_seq1	524	-0,49	3908	mating response MAPKKK (mating)
comp133634_c0_seq1	202	0,61	2122	mating factor receptor-coupled G protein (mating)
comp136211_c0_seq1	104	-0,61	470	Ribosomal large subunit pseudouridine synthase D (Swissprot)
comp1665_c0_seq1	69	0,92	795	Ankyrin-3 (Swissprot)
comp25626_c0_seq1	154	1,58	771	Histone H4 (Swissprot)
comp35751_c0_seq1	62	0,68	1498	Pentatricopeptide repeat-containing protein At5g25630 (Swissprot)
comp42918_c0_seq2	83	0,90	949	Phosphoenolpyruvate synthase (Swissprot)
comp54009_c0_seq1	363	0,73	1652	Heme oxygenase 1 (Swissprot)
comp54880_c0_seq1	66	-0,73	593	Uncharacterized protein ycf45 (Swissprot)
comp64328_c0_seq1	70	0,80	655	Ribulose biphosphate carboxylase (Swissprot)
comp65560_c1_seq1	147	1,80	618	MOB kinase activator-like 1 (Swissprot)
comp75076_c1_seq1	107	-1,80	532	JEM1p DnaJ-like chaperone required for nuclear membrane fusion during mating (mating)
comp75209_c0_seq1	139	-2,18	1780	SET and MYND domain-containing protein DDB_G0292454 (Swissprot)
comp82904_c0_seq1	234	0,51	1001	GDT1-like protein 3 (Swissprot)
comp83927_c1_seq1	121	1,22	819	Protein aardvark (Swissprot)
comp84842_c0_seq1	93	1,44	1193	Uncharacterized protein L662 (Swissprot)
comp92889_c0_seq1	490	0,54	1487	Omega-amidase NIT2 (Swissprot)
comp93025_c0_seq1	109	-0,60	704	Elongation factor P (Swissprot)
comp95901_c0_seq1	93	1,54	1115	Mucin-19 (Swissprot)
comp98445_c0_seq1	243	1,79	1903	Ankyrin-2 (Swissprot)
comp98462_c1_seq1	350	2,97	1300	MOB kinase activator-like 1 (Swissprot)
comp98485_c0_seq2	122	-0,75	1495	Putative pirin-like protein At3g59260 (Swissprot)
comp99456_c0_seq1	280	-0,66	1281	Glycerate dehydrogenase (Swissprot)

428

429

430

431 Table 2: Annotated transcripts DE between strains displaying opposite mating types and which crosses lead to the formation of resting cysts

Transcripts	Average expression	fold change (log ₂ (MT+/MT-))	Length	Homolog
comp104439_c0_seq1	248	-0,90	1061	Probable phytanoyl-CoA dioxygenase (Swissprot)
comp120943_c0_seq2	265	0,58	2335	Pentatricopeptide repeat-containing protein At2g41720 (Swissprot)
comp123246_c1_seq1	351	0,54	2014	Calcium-dependent protein kinase 24 (Swissprot) M96 mating-specific protein family (mating)
comp129407_c0_seq1	129	-0,78	1654	FAD-containing monooxygenase EthA (Swissprot)
comp129414_c0_seq1	127	0,62	1203	Aldose reductase B (Swissprot)
comp132997_c0_seq1	103	0,60	3288	Probable helicase A859L (Swissprot)

432

433

434

435

436

437

438

439

440

441

442

443

444

445

446

447

448

449

450

451

452

453

454

455

456

457

458

459 Figure legends:

460 Figure 1: Simplified *Alexandrium minutum* life cycle (adapted from Walker, 1984). Haploid vegetative cells divide by mitosis in the water column,
461 sexually compatible cells may fuse leading to the formation of a diploid planozygote that encysts as a resting cyst in the sediment. Following a
462 dormancy period, excystment and meiosis lead to the formation of new haploid vegetative cells.

463

464 Figure 2: Experimental design. A. Analyses performed. Cells are initially mixed at day 0. RNAseq analyses are performed at day 2 (when first
465 gamete fusions are observed) and day 5 (when first resting cysts are observed). Resting cysts are quantified at day 10 using inverted optic
466 microscopy. B. Pairwise crosses between four strains (Am231, Am233, Am1106, Am1249) with genetic group (GG) and mating type (MT) of the
467 strains indicated. C. Graphic summary of the five types of DE analyses performed and corresponding to the contact (1), Day 2 vs Day 5 (2),
468 Compatibility Day 2 (3) , Compatibility Day 5 (4), and strain (5) statistical analyses (see Material and Methods and Supplementary Table 3).

469

470 Figure 3: Resting cyst quantification performed at day 10 for the six pairwise crosses. At day 0, the initial density of each strain was 2,500 cell per
471 ml.

472

473 Figure 4: Overall variability of gene expression. First two axes of a PCA analysis on the entire gene expression dataset. Colors indicate the strains
474 involved and symbols specify whether it corresponds to a clonal sample or to a pairwise cross sampled after two or five days.

475

476 Figure 5: MA plots indicating, for each pair of strains, the difference in expression (log₂ fold change) between clonal controls and pairwise
477 crosses after two days. Each dot corresponds to a transcript, significant DE transcripts, if any, are in red.

478

479 Figure 6: MA plots indicating, for each pair of strains, the difference in expression (\log_2 fold change) after two days and five days. Each dot
480 corresponds to a transcript, significant DE transcripts are in red.

481

482 Figure 7: MA plots indicating the difference in expression (\log_2 fold change) between sexually compatible and incompatible crosses after two
483 days and five days. Each dot corresponds to a transcript, significant DE transcripts are in red.

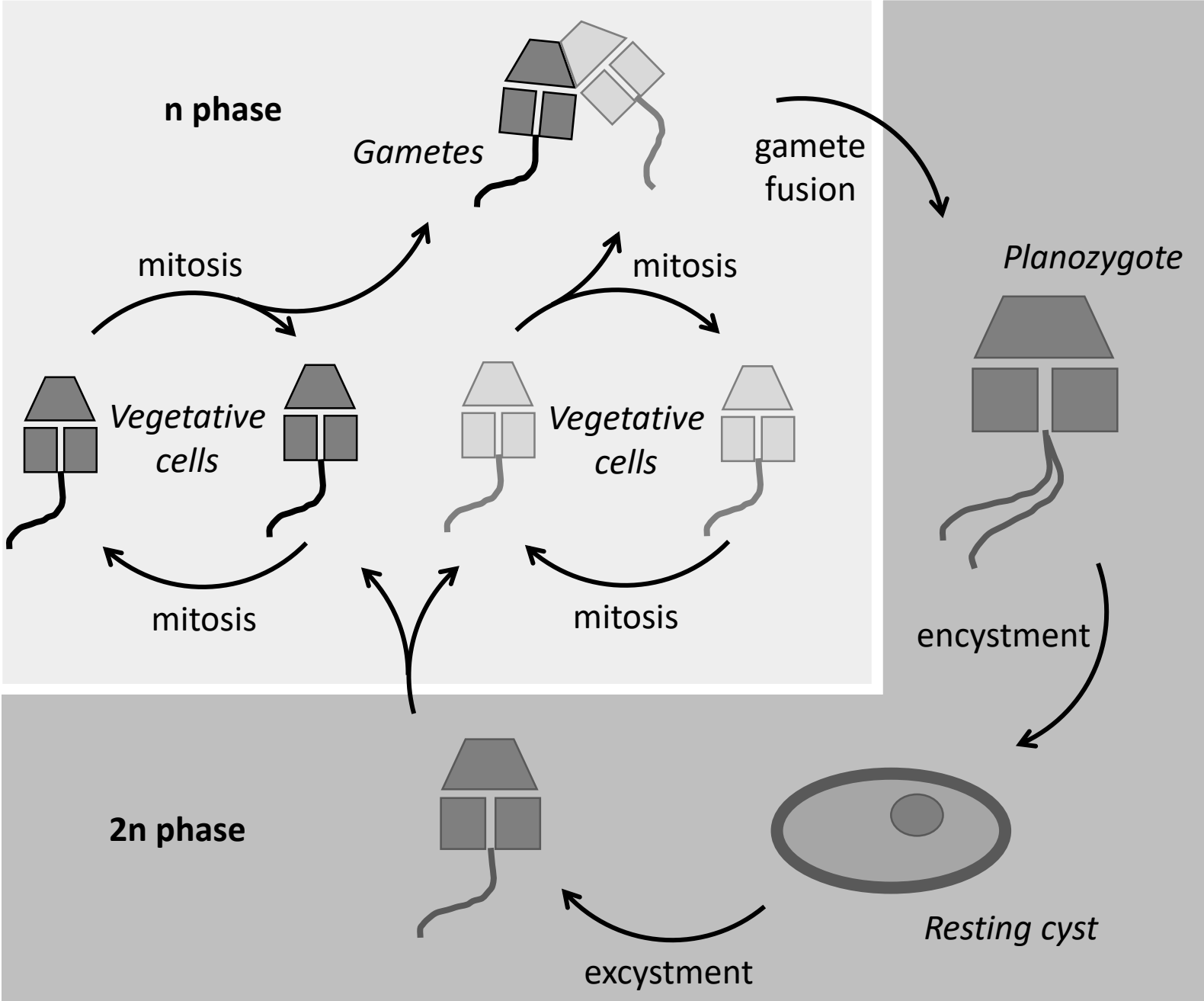
484

485 Figure 8: MA plots indicating the difference in expression (\log_2 fold change) between strains. Each dot corresponds to a transcript, significant DE
486 transcripts are in red. The number of significant transcripts is indicated.

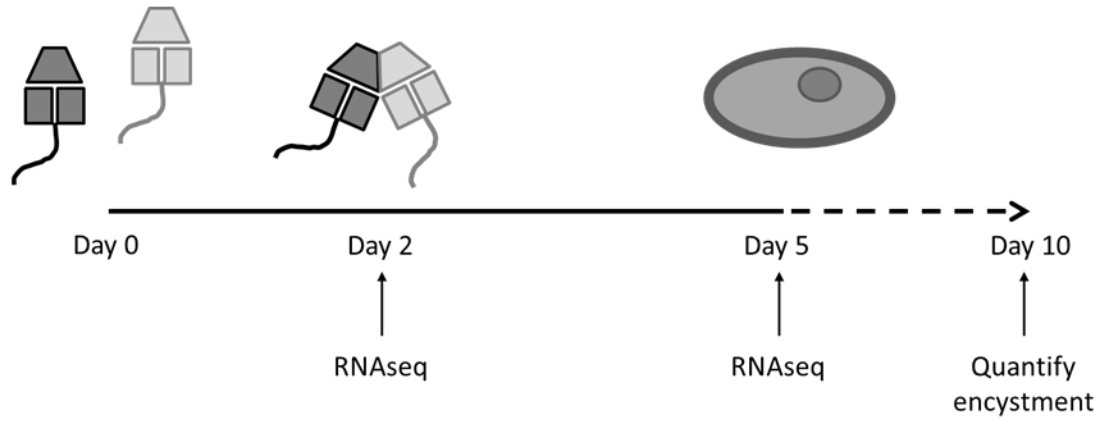
487

488 Figure 9: Overlap between sets of transcripts DE between strains. The total number of transcripts DE between pair of strains is represented on
489 the left barplot. The intersections displaying more than 150 transcripts are represented by the bottom plot, and the number of transcripts in
490 each intersection is shown on the top barplot. The orange barplot indicates the number of transcripts systematically DE between strains
491 belonging to genetic group A and B. The red barplot indicates the number of transcripts systematically DE between strains belonging to mating
492 type + and -. The purple barplots indicate the number of transcripts displaying strain specific DE.

493



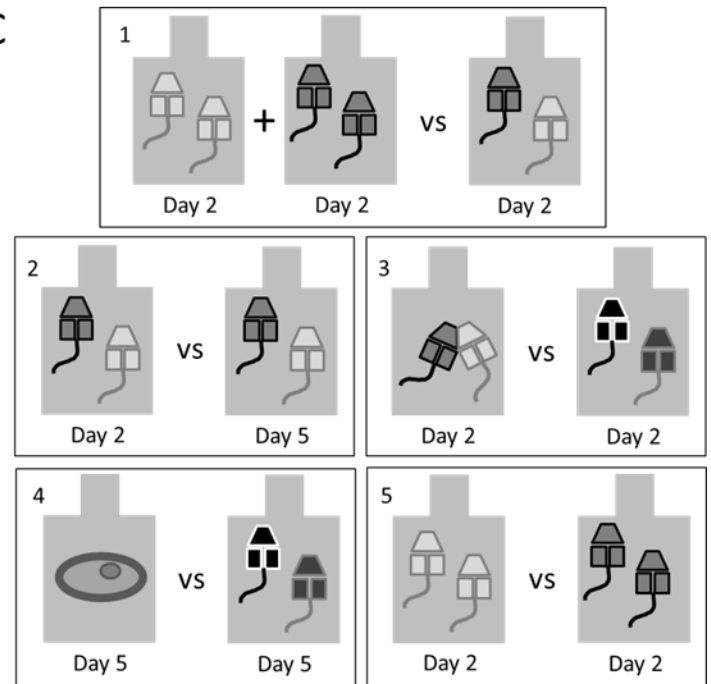
A

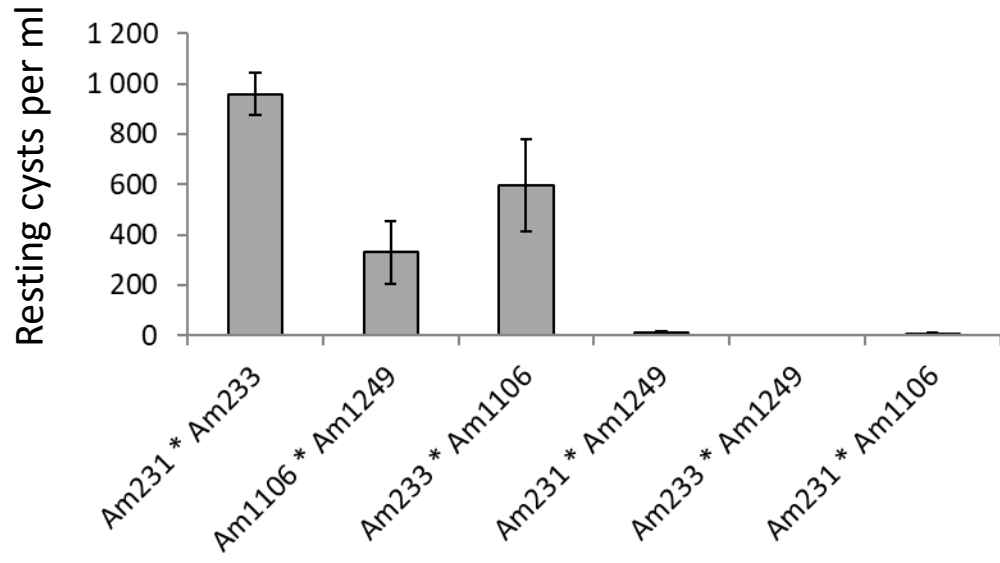


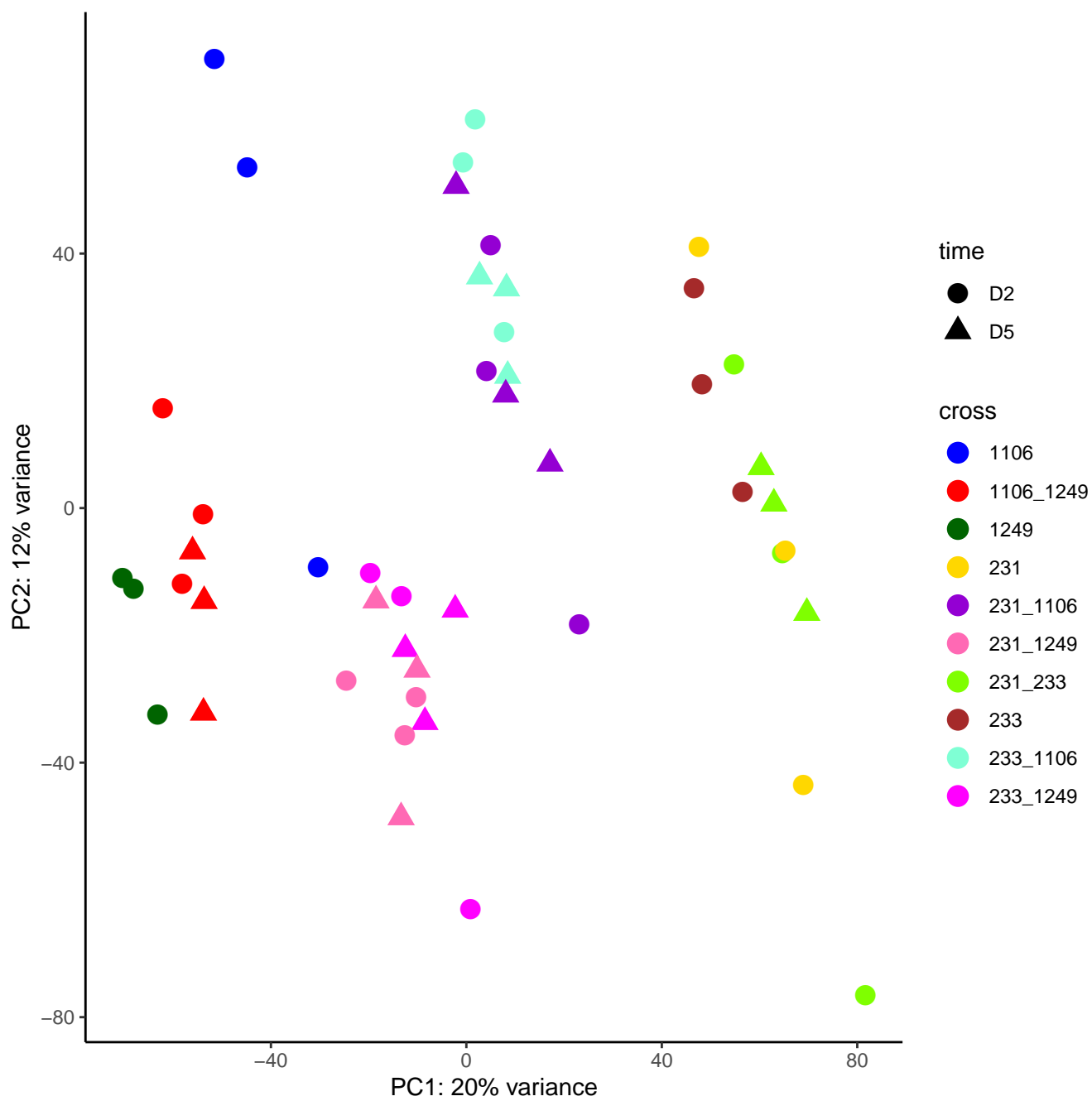
B

Am231	Am233	Am1106	Am1249	Strains	
				GG/MT	
B/+	B/-	A/+	A/-	GG/MT	
Clonal	intra-GG inter-MT	Inter-GG Intra-MT	Inter-GG Inter-MT	B/+	Am231
	Clonal	Inter-GG Inter-MT	Inter-GG Intra-MT	B/-	Am233
		Clonal	intra-GG inter-MT	A/+	Am1106
			Clonal	A/-	Am1249

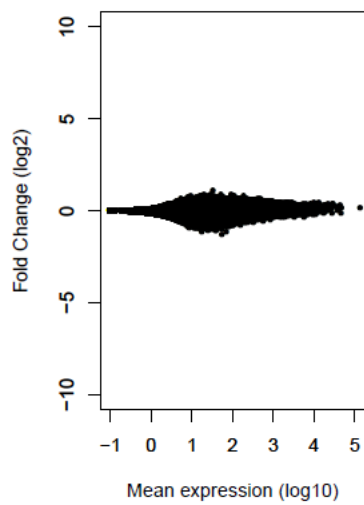
C



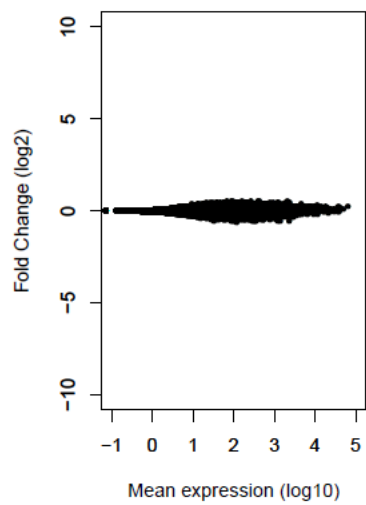




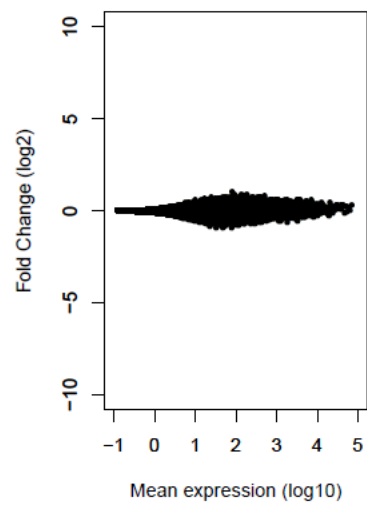
Am231 Am233



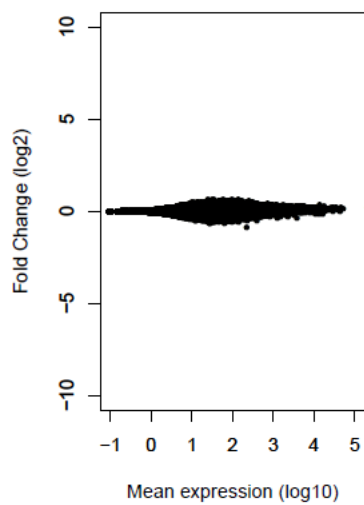
Am1106 Am1249



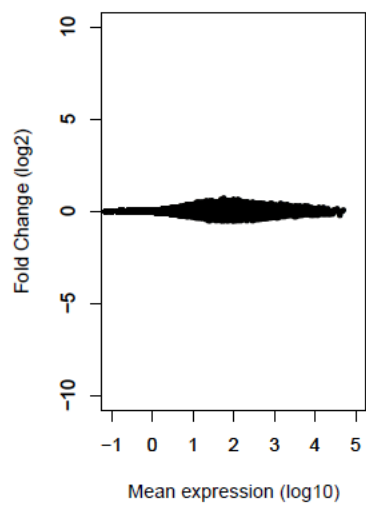
Am233 Am1249



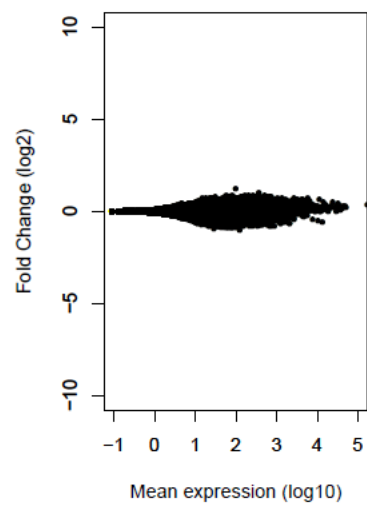
Am231 Am1106



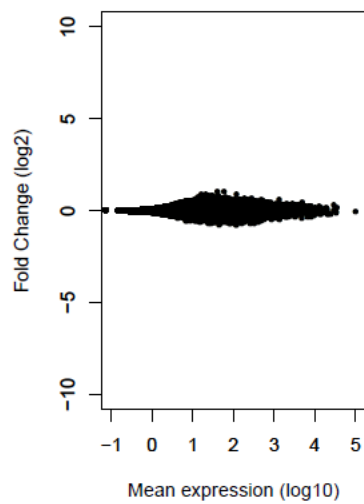
Am233 Am1106



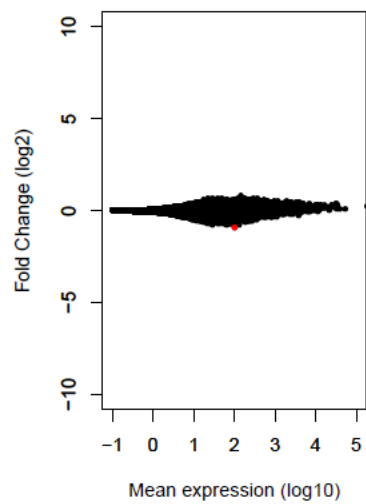
Am231 Am1249



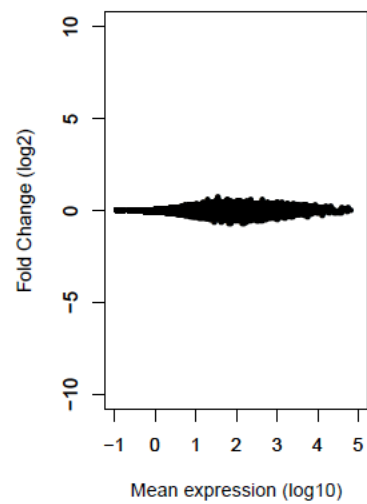
Am231 Am233



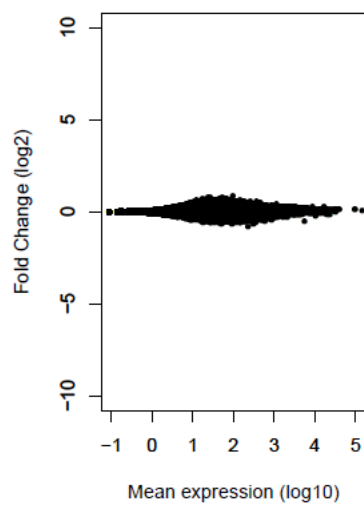
Am1106 Am1249



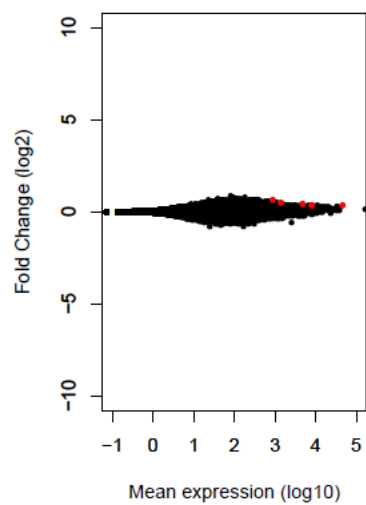
Am233 Am1249



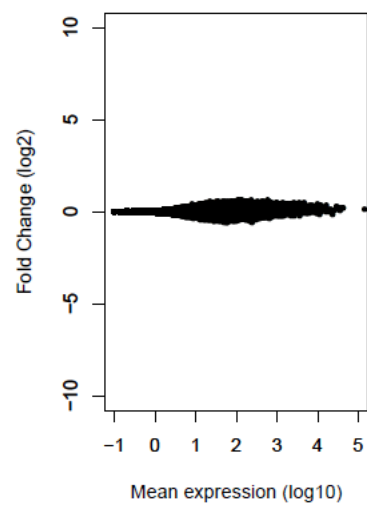
Am231 Am1106



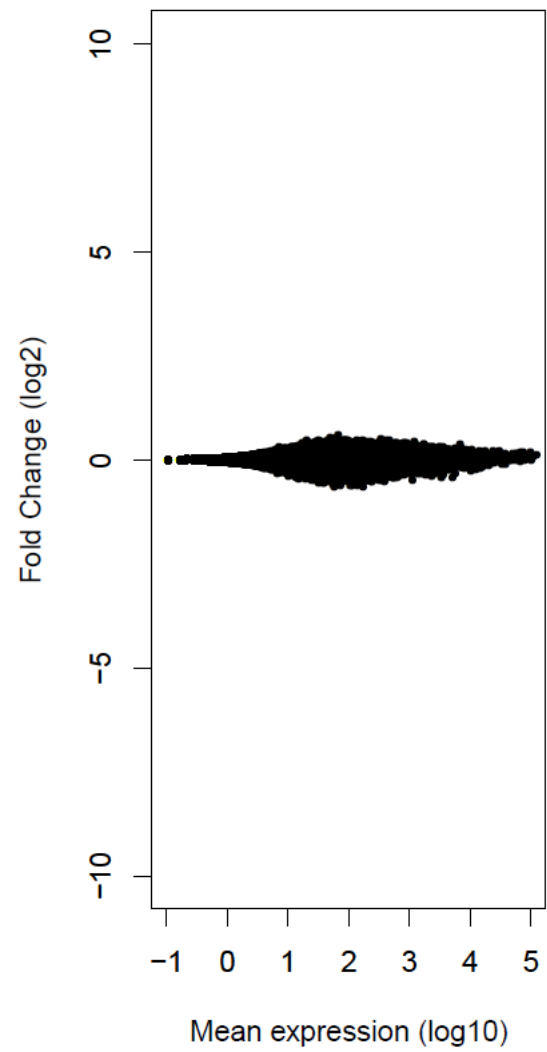
Am233 Am1106



Am231 Am1249



2 days



5 days

